BULLETIN OF THE POLISH ACADEMY OF SCIENCES
TECHNICAL SCIENCES, Vol. 60, No. 1, 2012
DOI: 10.2478/v10175-012-0010-0

Performance analysis of the sensorless adaptive sliding-mode neuro-fuzzy control of the induction motor drive with MRAS-type speed estimator

T. ORLOWSKA-KOWALSKA* and M. DYBKOWSKI

Institute of Electrical Machines, Drives and Measurements, Wroclaw University of Technology
19 Smoluchowskiego St., 50-372 Wroclaw, Poland

Abstract. This paper discusses a model reference adaptive sliding-mode control of the sensorless vector controlled induction motor drive in a wide speed range. The adaptive speed controller uses on-line trained fuzzy neural network, which enables very fast tracking of the changing speed reference signal. This adaptive sliding-mode neuro-fuzzy controller (ASNFC) is used as a speed controller in the direct rotor-field oriented control (DRFOC) of the induction motor (IM) drive structure. Connective weights of the controller are trained on-line according to the error between the actual speed of the drive and the reference model output signal. The rotor flux and speed of the vector controlled induction motor are estimated using the model reference adaptive system (MRAS) – type estimator. Presented simulation results are verified by experimental tests performed on the laboratory-rig with DSP controller.

Key words: electrical drive, induction motor, adaptive control, sliding mode control, neuro-fuzzy control, sensorless control.

1. Introduction

In modern industrial drives a requirement of high dynamical performance, consisting in perfect tracking or getting the reference signal with high dynamics and well damped transients is often met. This is especially important in servodrives [1–3]. Linear control theory not always gives satisfactory results in the design of effective control algorithms for such drive systems. Besides the drive system dynamics usually changes with the operating point and drive parameters change in a wide range depending on the system operation mode. For electrical drives this problem arises especially due to motors' winding temperature and saturation changes, as well as due to the drive inertia changes under system operation. So the development of the controller insensitive to those changes can enable high precision of the rotor speed control. One of the most popular control methods of the AC drives, witch is more robust to motor parameter changes, is a fuzzy-logic based control or adaptive control [4–7].

In [6] the PI type adaptive neuro-fuzzy speed controller (ANFC) for the sensorless induction motor (IM) drive system has been presented. In this paper, the adaptive PI-type controller is replaced with the adaptive sliding-mode neuro-fuzzy controller (ASNFC), with on-line learning capability [8].

Recently remarkable efforts have been made to develop state variables reconstruction of the induction motor (IM), such as rotor or stator flux vectors, motor electromagnetic torque and rotor speed, in order to obtain speed sensorless drive systems [1–3, 9, 10]. Applying of the flux and speed estimators or observers, significantly raises reliability and reduces costs of the induction motor drive. This is because of removing sensors that are mostly electromechanical parts.

Various methods of the rotor flux and speed estimation have been recently used, like physical, neural and algorithmic methods [9]. These last, based on the IM mathematical model are the most popular recently. Among algorithmic methods the concept based on the MRAS system, introduced by [11] and then modified by other authors [12, 13] or the full-order observer applied in model-reference structure introduced by [14, 15] seems to be relatively simple and interesting. However these estimators are sensitive to motor parameter changes due to the high sensitivity of current and voltage models used for the rotor flux vector estimation [16, 17] and require additional parameter tuning methods [18, 19]. In this paper the modification of the classical MRAS speed estimator was applied, described in detail in [20].

The main goal of this paper was to show that the implementation of the adaptive sliding-mode neuro-fuzzy controller (ASNFC), with on-line tuned parameters, in combination with the modified MRAS^{CC} speed and flux estimator, enables very good static and dynamic performance of the sensorless drive system (perfect tuning of the speed reference values, fast response of the motor current and torque, high accuracy of speed regulation) in a wide speed range, from zero to the 150% of the nominal value.

The paper is organized as follows. After short introduction, the developed sensorless adaptive control structure for the IM drive is described in Sec. 2. The algorithm for ASNFC is discussed and mathematical model of the MRAS^{CC} is presented, as well as its properties are shortly characterized. In the next two sections simulation and experimental results of

*e-mail: teresa.orlowska-kowalska@pwr.wroc.pl

the proposed sensorless control structure are shown, respectively. The dynamical performance analysis of the sensorless drive system with ASNF speed controller is performed from the point of view its proper operation in the normal speed range as well as in the low speed region, which usually is critical for classical drive control structure solutions.

2. Sensorless adaptive control structure

2.1. Adaptive sliding-mode neuro-fuzzy speed controller. The classical PI speed controller, usually applied in the DR-FOC structure of the IM drive (with the decoupling circuit [2, 9]), is replaced in this study by the ASNFC, tuned on-line in the model reference adaptive structure, as it is shown in Fig. 1.

The tracking error signal e_m between the desired output ω_{mod} of the reference model and the estimated speed of the drive system ω_m^e is used as a tuning signal. Control rules are tuned so that the actual output of the drive can follow the output of the reference model.

The general scheme of the used ASNFC is presented in Fig. 2a. It describes the relationship between the speed error $e(k)$, its change $\Delta e(k)$ and the change of the control signal $\Delta u(k)$. This fuzzy controller can be regarded as of PD-type. However, the control surface of the fuzzy system can be also seen as the nonlinear switching function [8], so this controller can be also regarded as the fuzzy sliding-mode controller (FSC), as it is in the present study.

According to the literature, two main frameworks of the fuzzy sliding mode control can be distinguished [5, 8]. In the first one the switching surface s is calculated directly. Then, on the basis of the obtained function s, the nonlinear switching function is approximated by the fuzzy system. The second framework is presented in detail in book [21] and used in this paper. In this approach the switching surface is not directly visible. It can be calculated from the properties of the rule base, which describe the relationship between the error (e) and the change of the error (Δe). Similarly to the classical sliding mode control, the switching surface is described by:

$$s^* = \lambda^* e^* + \Delta e^*, \tag{1}$$

where λ^* represents the slope of the switching line $\lambda^* e^* + \Delta e^* = 0$. The parameter λ^* can be calculated on the basis of the range of the universe of discussion of the input variable (e, Δe).

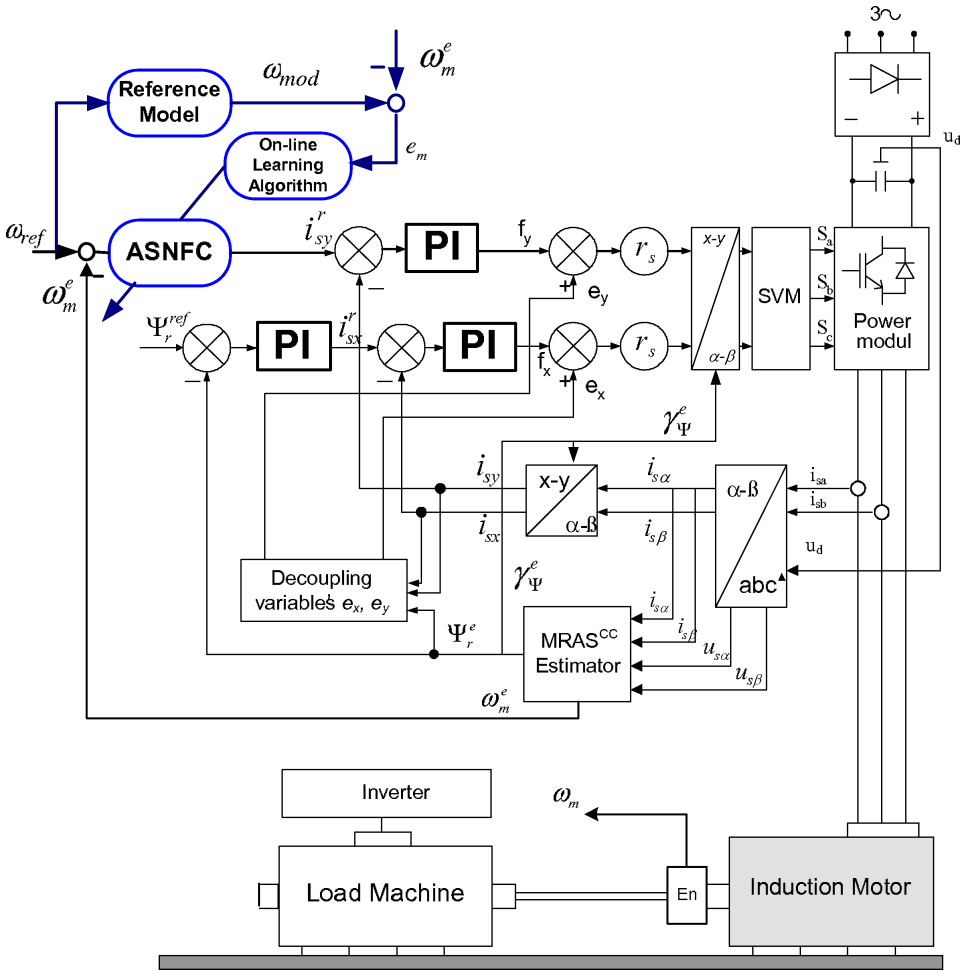

Fig. 1. Schematic diagram of the adaptive speed control structure for the field oriented control of the IM drive

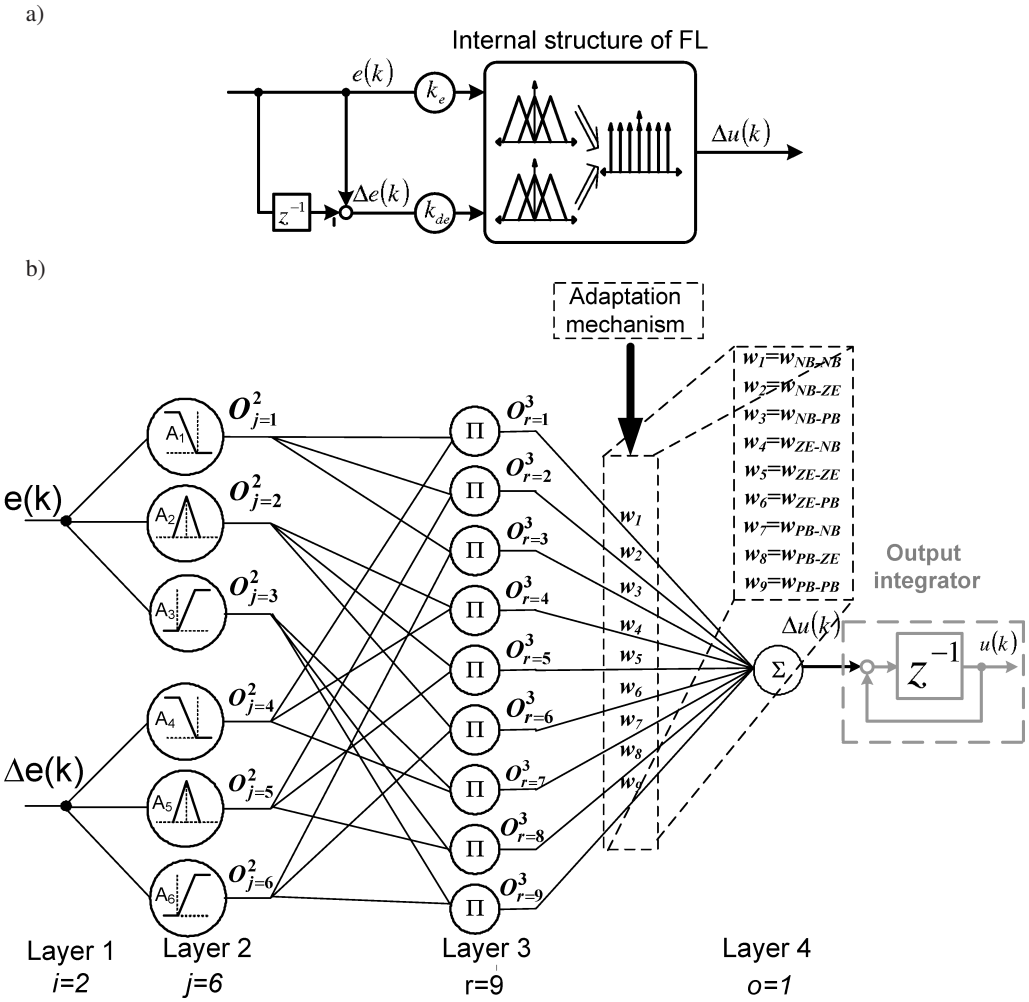

Fig. 2. A general structure of PD-type or sliding fuzzy controller (a) and its detail representation (b) (PD-type or sliding FL – solid line; PI-type after Ref. 6 – including dotted line)

The rule base of the fuzzy controller incorporates several *IF-THEN* rules, in the following form:

$$R_j: \ IF\ x_1 \text{ is } A_1^j \text{ and } x_2 \text{ is } A_2^i \ THEN\ y = w_i, \qquad (2)$$

where x_i – input variable of the system, A_i^j – input membership function, w_i – consequent function.

This controller can be realized as a general structure of neuro-fuzzy system shown in Fig. 2b [5, 8, 21]. Moreover in this figure the difference between PI and PD (or sliding) type of the controller is shown.

The functions of each layer are presented as follows:

Layer 1. Each input node in this layer corresponds to the specific input variable ($x_1 = e(k)$; $x_2 = \Delta e(k)$). These nodes only pass input signals to the second layer.

Layer 2. Each node performs a membership function O_i^2, that can be referred to as the fuzzification procedure.

Layer 3. Each node in this layer represents the precondition part of fuzzy rule and is denoted by Π which multiplies the incoming signals and sends the results out.

Layer 4. This layer acts as a defuzzifier. The single node is denoted by Σ and sums of all incoming signals. A defuzzification process in the neuro-fuzzy network, known as the singleton defuzzification method, is described by:

$$\Delta u = y_o = \sum_{j=1}^{M} w_j O_j^3. \qquad (3)$$

In this paper sliding neuro-fuzzy controllers with 9 rules and triangular membership functions, shown in Fig. 2 is tested (solid line), opposite to the paper [6], where PI-type NFC (including doted line) was applied. The fuzzy controller is tuned so that the actual motor speed ω_m^e of the sensorless drive system can follow the output of the reference model ω_{mod} (see scheme in Fig. 1a). The tracking error is used as the tuning signal. The reference model is chosen as a standard second order term [6, 8]:

$$G_m(s) = \frac{\omega_n^2}{s^2 + 2\zeta\omega_n s + \omega_n^2}, \qquad (4)$$

where ζ is a damping ratio and ω_n is a resonant frequency.

The supervised gradient descent algorithm is used to tune the parameters $w_1, \ldots, w_M$ in the direction of minimizing the cost function like:

$$J(k) = \frac{1}{2}(\omega_{mod} - \omega_m^e)^2 = \frac{1}{2}e_m^2. \tag{5}$$

Parameter adaptation obtained using the modified algorithm based on local gradient PD control is used:

$$\begin{aligned} w_j(k+1) &= w_j(k) + \gamma\, \delta_o O_j^3 \\ &\cong w_j(k) + k_p e_m O_j^3 + k_d\, \Delta e_m, \end{aligned} \tag{6}$$

where Δe_m is the derivative of the e_m.

The derivative term is used to suppress a large gradient rate. The dynamic property of the drive system strictly depends on the value of the learning rates k_p, k_d. The maximum value which guarantees the convergence of the system can be obtained by the analysis of the discrete type Lyapunov function [4].

The other controllers of the DRFOC structure (Fig. 1) have been adjusted according to rules demonstrated e.g. in [23].

2.2. MRAS-type speed estimator. The main problem in the sensorless IM drive, is proper estimation of the rotor speed and the rotor flux vector – especially in the low speed region [9, 10]. State variable estimation methods used in the advanced drive system applications should be less sensitive to the drive nonlinearities and motor parameter uncertainties (e.g. parameter identification errors). So in the proposed high performance drive system, for the rotor flux and speed estimation the newly developed MRAS^{CC} estimator, proposed firstly in [17], characterized with very good stability and robustness to motor parameter changes is applied.

This MRAS^{CC} estimator is based on the comparison between the measured stator current of the induction motor and the estimated current obtained from the stator current model (Fig. 3). Such stator current model requires the information about the rotor flux vector. In the proposed MRAS^{CC} estimator this state variable is calculated based on the speed dependent current model of the rotor flux [2, 9]. Both stator current model:

$$\begin{aligned} \frac{d}{dt}\mathbf{i}_s^e &= -\frac{r_r x_m^2 + x_r^2 r_s}{\sigma \tau_N x_s x_r^2}\mathbf{i}_s^e + \frac{1}{\sigma \tau_N x_s}\mathbf{u}_s \\ &+ \frac{x_m r_r}{\sigma \tau_N x_s x_r^2}\mathbf{\Psi}_r^i - j\omega_m^e \frac{x_m}{\sigma \tau_N x_s x_r}\mathbf{\Psi}_r^i \end{aligned} \tag{7}$$

and rotor flux model:

$$\frac{d}{dt}\mathbf{\Psi}_r^i = \left[\frac{r_r}{x_r}(x_M \mathbf{i}_s - \mathbf{\Psi}_r^i) + j\omega_m^e \mathbf{\Psi}_r^i\right]\frac{1}{\tau_N} \tag{8}$$

are adjusted by the estimated rotor speed, according to the schematic diagram presented in Fig. 3.

The following notation is used in (7)–(8): ω_m^e –estimated rotor speed, r_s, r_r, x_s, x_r, x_m – stator and rotor resistances, stator and rotor leakage reactances, $\mathbf{u}_s$, $\mathbf{i}_s^e$, Ψ_r^i – stator voltage, estimated stator current and rotor flux vectors respectively, $\sigma = 1 - x_m^2/x_s x_r$. $\tau_N = 1/2\pi f_{sN}$.

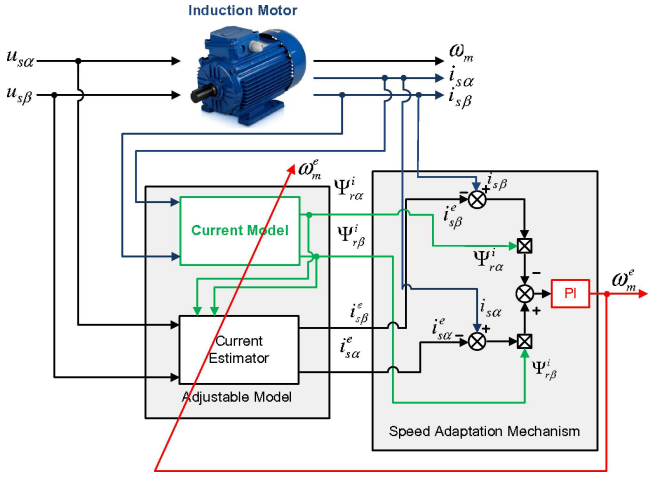

Fig. 3. Schematic diagram of the MRAS^{CC} estimator

The speed adjustment algorithm used in this MRAS^{CC} estimator is different from the classical solution and is based on the error between estimated and measured stator current, according to the formula used in the full-order flux observer with speed adaptation developed in [15]:

$$\begin{aligned} \omega_m^e &= K_P\left(e_{i_{s\alpha}}\Psi_{r\beta}^i - e_{i_{s\beta}}\Psi_{r\alpha}^i\right) \\ &+ K_I \int \left(e_{i_{s\alpha}}\Psi_{r\beta}^i - e_{i_{s\beta}}\Psi_{r\alpha}^i\right)\, dt, \end{aligned} \tag{9}$$

where $e_{i_{s\alpha,\beta}} = i_{s\alpha,\beta} - i_{s\alpha,\beta}^e$ – error between estimated and measured stator current, $\Psi_{r\alpha,\beta}^i$ – components of the rotor flux vector estimated by the rotor current model; K_P, K_I – coefficients, adjusted according to the stability analysis of the estimator [20].

The obtained rotor speed value is used in the current model of rotor flux and stator current estimator as changeable parameter, as shown in the Fig. 3.

The MRAS^{CC} estimator is more robust to the motor parameter changes than other adaptive estimators [17, 20], so the whole control structure with the adaptive sliding mode fuzzy neural network controller (ASNFC) supported with MRAS^{CC} estimator should be more robust to the motor parameter changes and load side inertia changes than classical sensorless drive with PI controller used in the speed control loop. Moreover this estimator is stable in the wide range of the rotor speed and can work properly in the sensorless control structure, which was proved under theoretical analysis as well as in simulation and experimental tests shown in [20].

3. Simulation results

The described sensorless control structure of the induction motor drive has been tested in simulation first, using MATLAB/Simulink®, for 1.5 kW IM drive (see Appendix for parameters). The most important problem in the sensorless drive system with IM is stability in the low speed region. So in this paper the simulation results for low speed region are demonstrated, in similar operation conditions as for previously tested IM drive with ANFC of PI-type speed controller, presented in [6], with an adaptive full order observer [14].

The one of goals of this paper is to show the advantages of the controller presented here, over the ANFC developed earlier [6]. The quality of reference speed tuning depends on k_d and k_p parameters of the adaptive law (6). The bigger values of these parameters cause the faster decrease of the system tracking error. However, too large values of adaptation coefficients introduce the high frequency oscillations into the system state variables. In order to select optimal values of k_d and k_p, the nominal parameters of the drive are assumed. Then parameters k_d and k_p were determined using off-line optimization (genetic) algorithm, to eliminate the tracking error as soon as possible.

In Fig. 4 all state variables transients of the sensorless IM drive and chosen weight factors of the ASNFC are demonstrated, and compared to the transients obtained for ANFC PI-type speed controller tested previously in [6]. The drive system with new controller performs much better, starting from the beginning of the weights adaptation process. The speed error is almost negligible, even in the first reverse operation period, on contrary to the previously tested adaptive ANFC of PI type. Very good tracking performances of the sensorless drive system are obtained, as well for nominal value of mechanical time constant τ_M as for the much bigger one. Transient speed errors occur (up to 5%÷10% pulse) only in the moment of very fast reference speed changes. It proves that the proposed ASNFC is very robust to drive inertia changes and can be implemented in the applications with such parameter changes.

In all sensorless drive systems the serious problems occur during zero speed crossing under full load. This situation was tested in simulations and obtained results are demonstrated in Fig. 5. Transients of the adaptive system during slow reverse of the speed reference with simultaneous step changes of the nominal load torque value are presented there. The speed tracking error is effectively damped by the ASNF controller and only very small speed overshoots occur in the moment of the load torque change (Fig. 5a). The sensorless adaptive drive system does not loose the stability under zero speed crossing and full load torque.

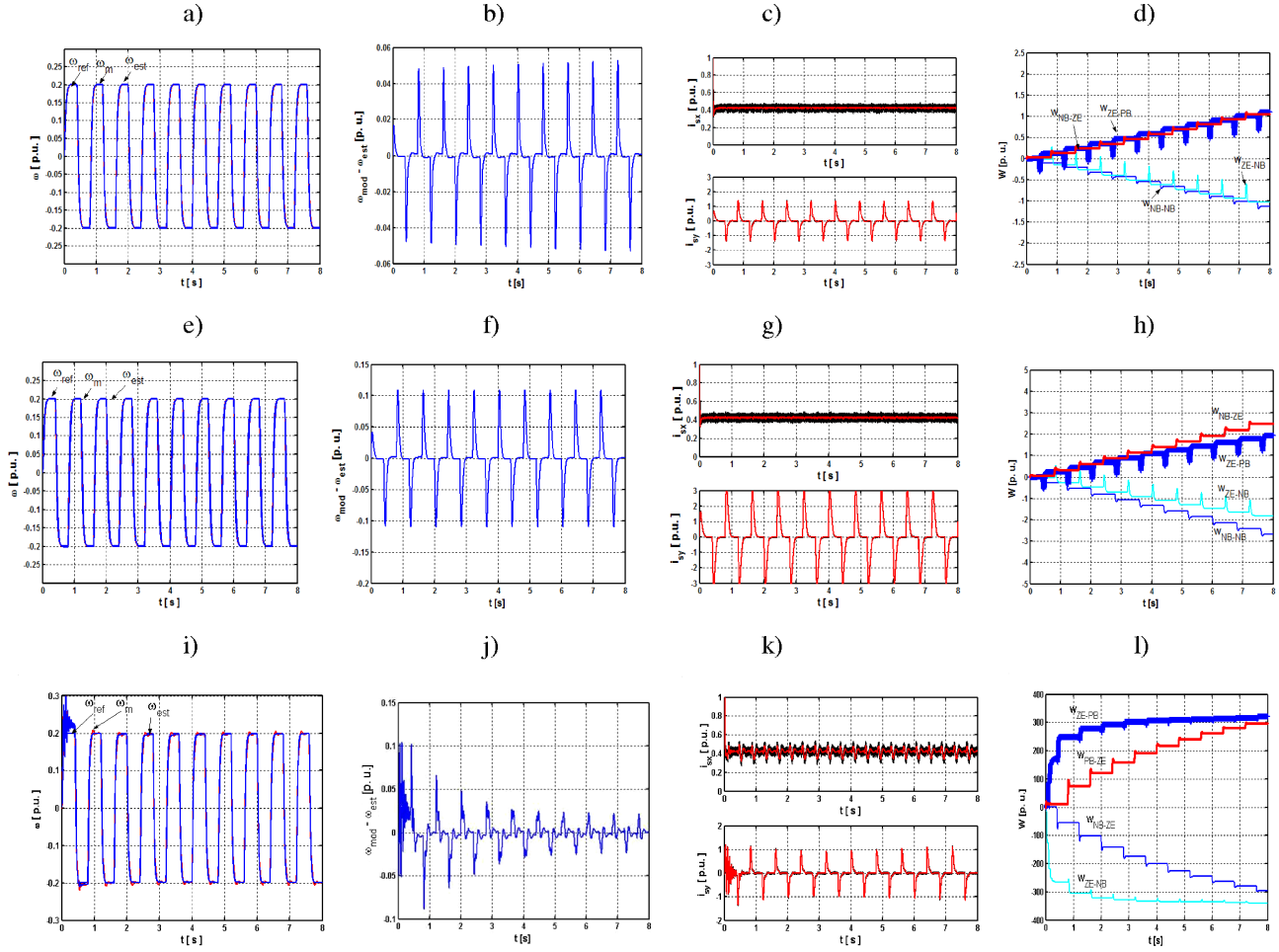

Fig. 4. Transients of the IM drive with ASNFC (a-f) and ANFC [6] (i-l) for the step changes of speed reference and $\tau_M = \tau_{MN}$ (a-d, i-l), $\tau_M = 3\tau_{MN}$ (e-h): (a,e,i) reference and estimated rotor speeds, (b,f,j) speed error, (c,g,k) stator current components, (d,h,l) chosen ASNFC weight factors w_i

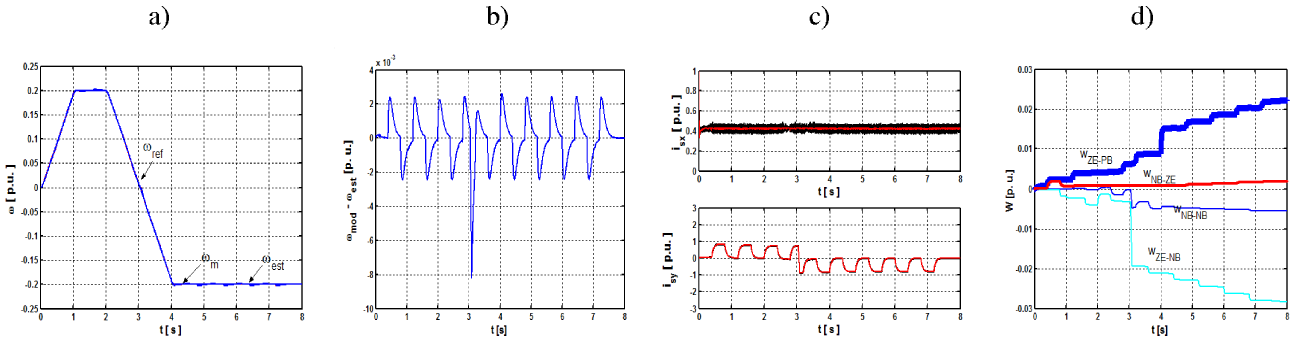

Fig. 5. Transients of the IM drive with ASNFC for slow reverse of the speed reference and step changes of load torque $T_L = 0 \rightarrow T_{LN}$: (a) reference and rotor speeds, (b) speed error, (c) stator current components, (d) chosen weight factors w_i

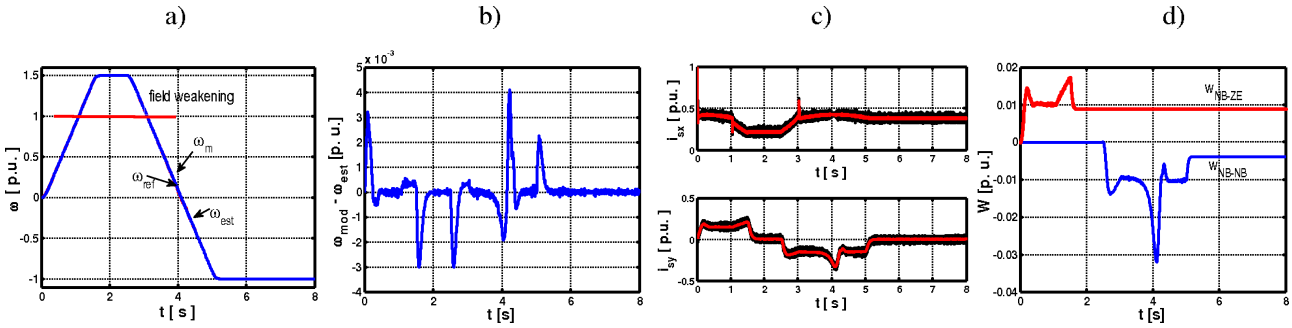

Fig. 6. Transients of the IM drive with ASNFC for long reverse operation from $1.5\omega_N$ to $-\omega_N$ (a) reference and rotor speeds, (b) speed error, (c) stator current components, (d) chosen ASNFC weight factors w_i

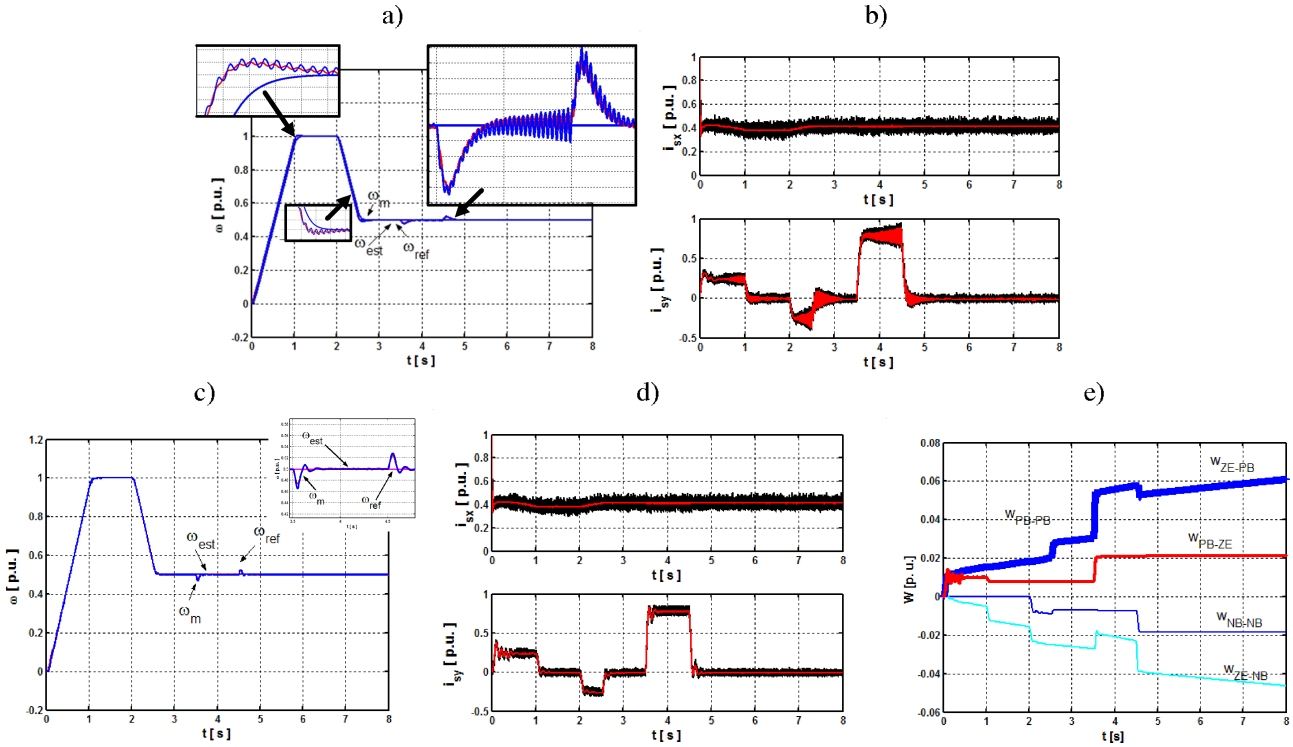

Fig. 7. Transients of the IM drive with PI controller (a, b) and with ASNFC (c, d, e) for wrong r_s identification ($r_s = 1.3r_{sN}$) (a, c) reference and rotor speeds, (b, d) stator current components, (e) chosen ASNFC weight factors w_i

In the Fig. 6 the similar long reverse operation is presented, but in a different speed range, including the field weakening (from 1.5 ω_N to – ω_N). It is seen that the drive system with ASNFC and MRAS^{CC} speed estimator is stable for the field weakening region and for zero speed operation. After the reverse operation the weight factors are constant. So it is proved in simulation that the proposed sensorless adaptive control structure can work stable in the wide range of the speed reference changes.

All well known speed and rotor flux estimators are sensitive to the motor parameter changes. MRAS^{CC} estimator is less sensitive to the motor parameter changes than other similar solutions, what was presented in detail in [20]. The proposed control structure with MRAS^{CC} estimator has been tested for the stator resistance r_s mismatch and obtained results are compared to the structure with the classical P speed controller (Fig. 7).

It can be seen in Fig. 7a, that even for the classical PI speed controller (with constant gains) the control structure is stable and works properly with wrong value of the stator resistance, but only for no-load condition. If load torque is different than zero, some small oscillations of the estimated speed are visible in such case, similarly as noticeable oscillations of the stator current component i_{sy}, which is responsible for the electromagnetic torque developed by the IM in the DRFOC structure. Thus for the loaded drive with PI speed controller and wrong identification of the stator winding resistance, not stable operation of the rotor speed and current i_{sy} can be observed. When the PI speed controller is replaced by the proposed ASNFC (Fig. c-d), controller adapts its parameters according to the adaptation rule (6) and tracks the reference speed with high accuracy, thus it compensates also the oscillations of the estimated speed (it should be mentioned that parameters K_I and K_P in the speed adaptation mechanism (9) of the MRAS^{CC} speed estimator are the same in both cases).

4. Chosen experimental results

The whole adaptive sensorless induction motor drive with MRAS^{CC} estimator has been implemented in the laboratory set-up with PC computer using the dSPACE 1103 software. The schematic diagram of the experimental test bench is shown in Fig. 8.

The experimental set-up is composed of the IM motor fed by the SVM voltage inverter. The motor is coupled to a load machine (AC motor supplied from an inverter). The driven motor has the nominal power of 1.5 kW. The speed and position of the drive are measured by the incremental encoder (36000 imp./rev – Kubler 580x), only for the comparison with the estimated speed in the sensorless drive system. The drive system operation was tested in various conditions, including idle-running with and without load, slow reverse under load and response of the system to reference speed and load torque changes.

In the following figures chosen experimental results are shown, where transient of the most important drive system variables are demonstrated in all figures (reference, measured and estimated speeds, speed errors, stator current components, rotor flux vector, chosen controller weight factors w_i).

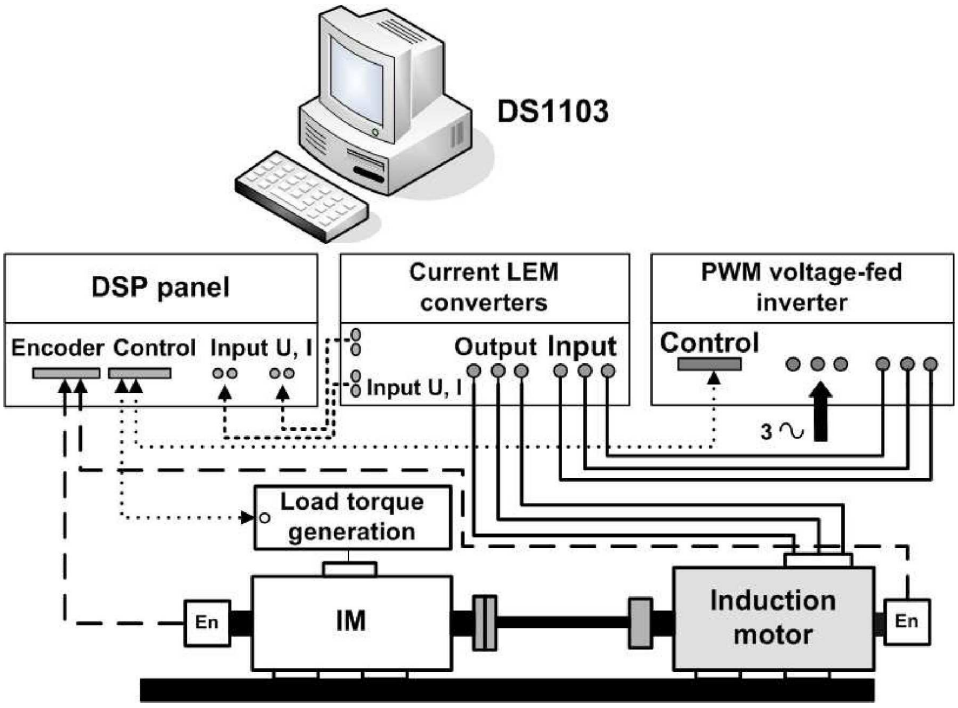

Fig. 8. Schematic diagram of the laboratory test bench

First, in Fig. 9 the operation of the sensorless drive system under changing load condition in relatively low speed region is shown (as in simulations; see Fig. 4). A very fast dumping of the speed overshoot under step changes of the load torque is observed (Fig. 9c). The changes of the stator current component i_{sy}, presented in Fig. 9d, show directly the step load torque changes of the drive system. Simultaneously the second component i_{sx} is proportional to the nominal rotor flux value, which is stabilized in the DRFOC structure.

To show the performance of the drive system under no-load zero speed operation, which is critical for the sensorless operation [22], transients for braking to zero speed from $\omega_{ref} = \pm 0.2\omega_N$ are presented in Fig. 10. It can be seen that the adaptation process of the speed controller performs very well (it starts from zero weights, as usually). Also the MRAS^{CC} estimator enables perfect tracking of the reference speed while the real speed differs from the estimated one only in the moment of sudden change of the reference value.

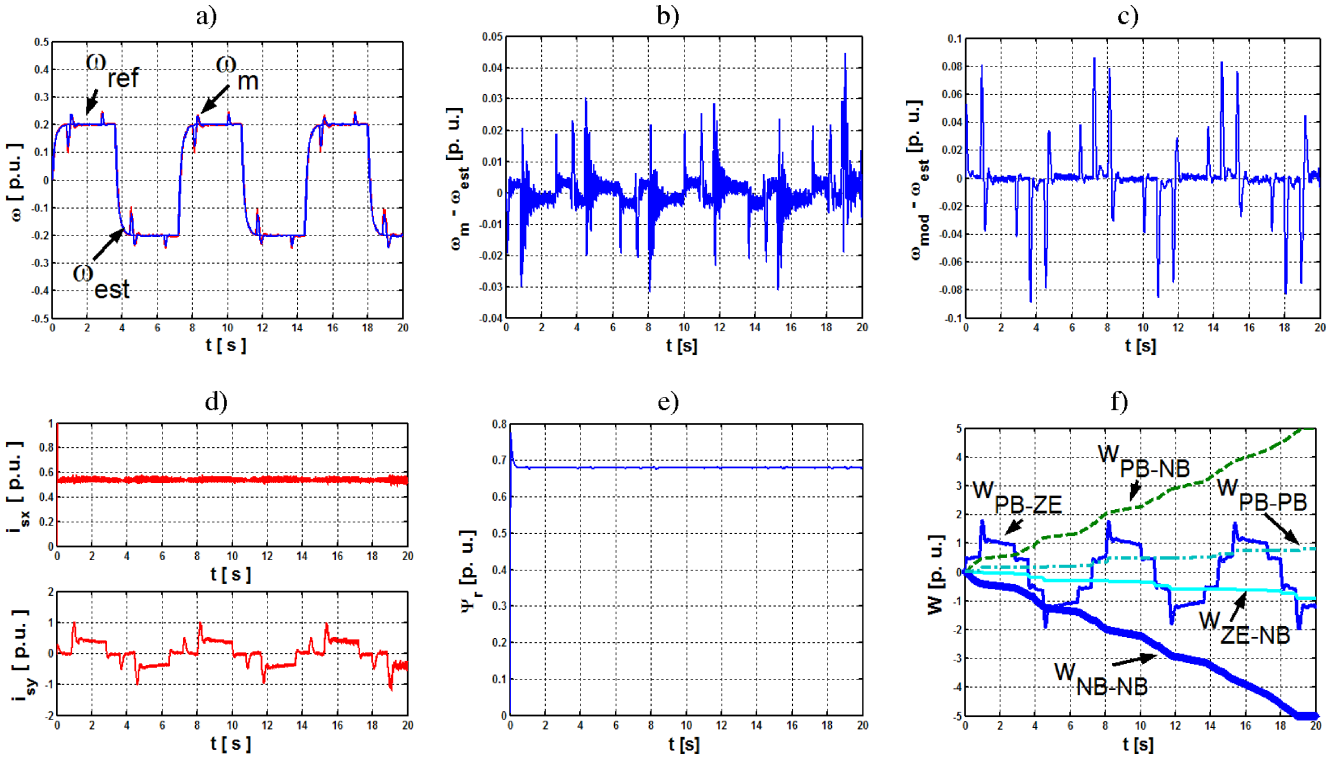

Fig. 9. Experimental transients of the IM drive with ASNFC for the constant speed reference $\omega_{ref} = 0.2\omega_N$ and $T_L = T_{LN}$

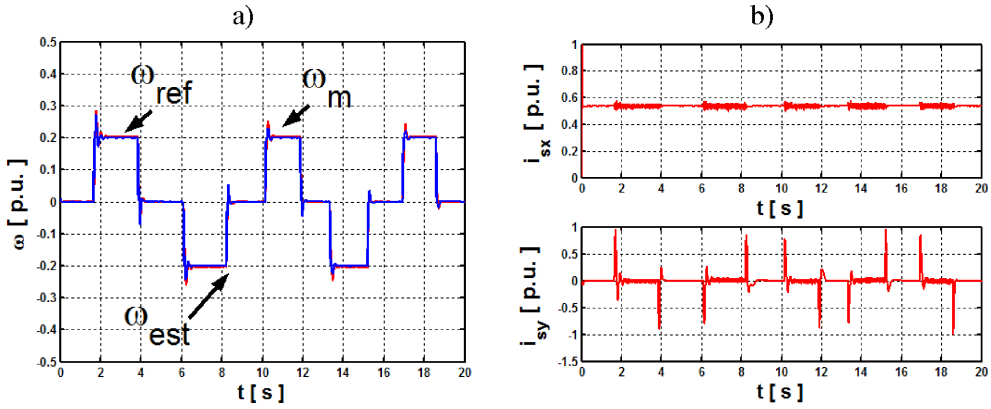

Fig. 10. Experimental transients of the IM drive with ASNFC for breaking to zero speed reference

Next, in Fig. 11 transients of the sensorless IM drive with ASNFC for cyclic reverse speed reference changes in a very low speed range ($\pm 0.05\omega_N$) and no-load operation are presented. The error between the measured and estimated speed oscillates around zero (Fig. 11b). The weights of the ASNFC are automatically adjusted and depend on the mechanical and electrical parameters of the tested structure (Fig. 11f). It can be seen that the weight adaptation process is stable. Rotor flux vector is constant, stator current components have proper shapes and values, according to the DRFOC concept and operation conditions of the drive system.

The sensorless induction motor drive with MRAS^{CC} speed and flux estimator and with the proposed adaptive sliding-mode neuro-fuzzy speed controller works properly for the idle-running and the load torque conditions in the wide range of speed reference changes (Fig. 9–11). The behavior of the real drive system confirms all theoretical results obtained in simulations.

5. Conclusions

The sensorless IM drive with a model reference adaptive speed control using on-line trained sliding-mode neuro-fuzzy controller is presented in the paper. The structure and on-line learning algorithm of ASNF is described. The performances of the proposed system have been illustrated by simulation and experimental results. The simulations have confirmed the efficiency of the proposed adaptive scheme for control of the sensorless IM without use of any qualitative knowledge about the plant parameters. An adaptive controller can deal with large range of drive parameter variations and external disturbance due to its on-line learning capability. The MRAS^{CC} speed and rotor flux estimator has ensured very good accuracy of the rotor speed estimation, which has resulted in proper operation of the drive system in the low speed range, under idle-running and load torque changes, for fast and slow changes of the speed reference value. The behavior of the real drive system confirms all theoretical results obtained in simulations and proves better performance of the ASNF speed controller over the PI-type ANFC tested previously in [6] for the IM drive.

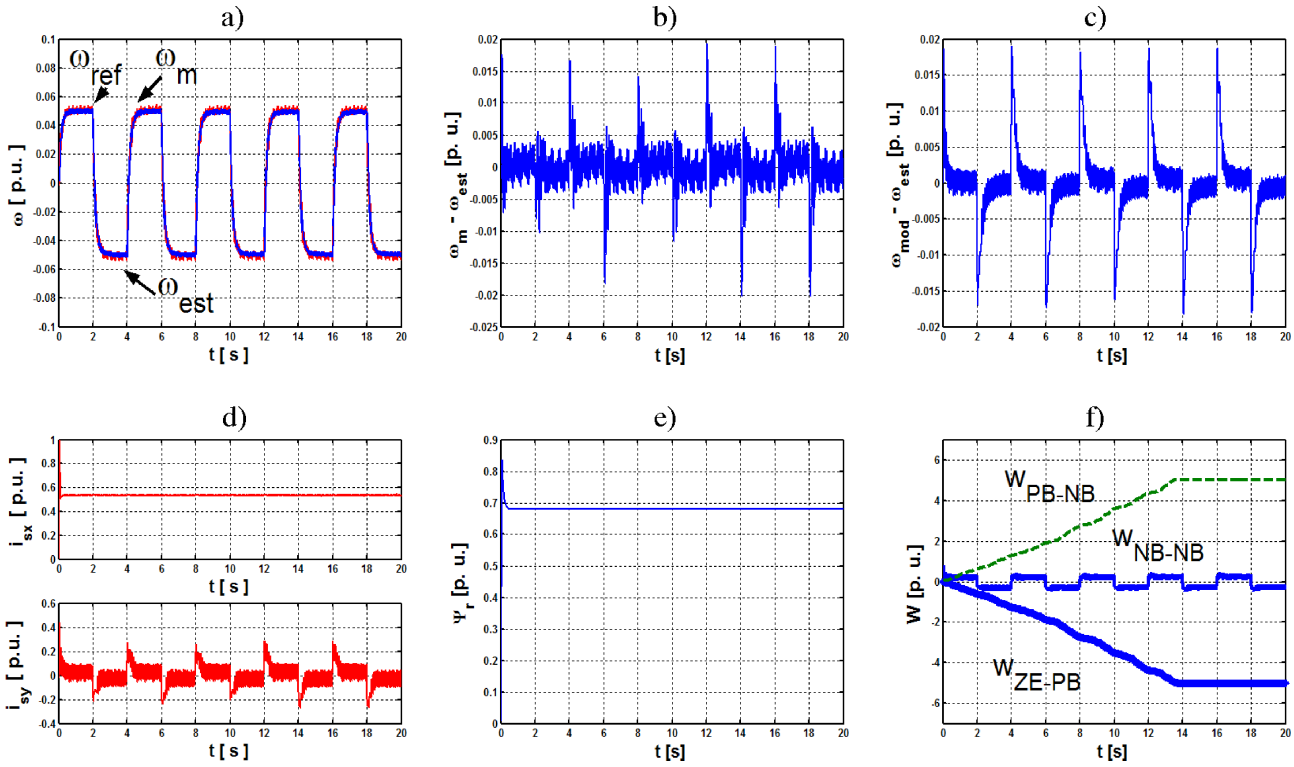

Fig. 11. Experimental transients of the IM drive for the reverse operation at low speed reference ($\pm 0.05\omega_N$) and $T_L = 0$

Appendix

Motor Data:

Rated values		Parameters: $\tau_M = 0.0188$ [s]					
$P_N = 1.5$ [kW]	$n_N = 2820$ [rpm]	R_s	R_r	X_s	X_r	X_m	
$U_N = 230/400$ [V]	$f_N = 50$ [Hz]	3.68	4.033	119.93	119.93	115.77	[Ω]
$I_N = 5.9/3.4$ [A]	$p_b = 3$	0.0543	0.0595	1.769	1.769	1.7076	[p.u.]

REFERENCES

[1] P. Vas, *Sensorless Vector and Direct Torque Control*, Oxford University Press, New York, 1998.

[2] M.P. Kazmierkowski, F. Blaabjerg, and R. Krishnan, *Control in Power Electronics – Selected Problems*, Academic Press, New York, 2002.

[3] J.W. Finch and D. Giaouris, "Controlled AC electrical drives", *IEEE Trans. Industrial Electronics* 55 (2), 481–491 (2008).

[4] F.J. Lin, R.F. Fung, and R.J. Wai, "Comparison of sliding-mode and fuzzy neural network control for motor-toggle servomechanism", *IEEE Trans. Mechatronics* 3 (4), 302–318 (1998).

[5] F.J. Lin, C.H. Lin, and P.H. Shen, "Self-constructing fuzzy neural network speed controller for permanent-magnet synchronous motor drive", *IEEE Trans. on Fuzzy Systems* 9 (5), 751–759 (2001).

[6] T. Orlowska-Kowalska, M. Dybkowski, and K. Szabat, "Adaptive neuro-fuzzy control of the sensorless induction motor drive system", *12th Int. Power Electronics and Motion Control Conf. EPE-PEMC'2006* 1, 1836–1841 (2006).

[7] T. Orlowska-Kowalska and K. Szabat, "Control of the drive system with stiff and elastic couplings using adaptive neuro-fuzzy approach", *IEEE Trans. Ind. Electronics* 54 (1), 228–240 (2007).

[8] T. Orlowska-Kowalska and K. Szabat, "Damping of torsional vibrations in two-mass system using adaptive sliding neuro-fuzzy approach", *IEEE Trans. Industrial Informatics* 4 (1), 47–57 (2008).

[9] T. Orlowska-Kowalska, *Sensorless Induction Motor Drives,* Wroclaw University of Technology Press, Wroclaw, 2003.

[10] J. Holtz, "Sensorless control of induction machines – with or without signal injection?", *IEEE Trans. Ind. Electronics* 53 (1), 7–30 (2006).

[11] S. Tamai, H. Sugimoto, and Y. Masao, "Speed sensorless vector control of im with model reference adaptive system", *IEEE Industry Appl. Society 27th Annual Meeting IAS'1987* 1, 189–195 (1987).

[12] S.C. Schauder, "Adaptive speed identification for vector control of induction motors without rotational transducers", *IEEE Trans. Industry Applications* 28 (5), 1054–1061 (1992).

[13] M. Rashed and A.F. Stronach, "A stable back-EMF MRAS-based sensorless low-speed induction motor drive insensitive to stator resistance variation", *IEEE Proc. – Electric Power Applications* 151 (6), 685–693 (2004).

[14] M. Morawiec, Z. Krzeminski, and A. Lewicki, "Voltage multi-scalar control of induction machine supplied by current source converter", *IEEE Int. Symposium on Industrial Electronics (ISIE)* 1, CD-ROM (2010).

[15] H. Kubota, K. Matsuse, and T. Nakano, "DSP-based speed adaptive flux observer of induction motor", *IEEE Trans. Industry Applications* 29 (2), 344–348 (1993).

[16] T. Orlowska-Kowalska, P. Wojsznis, and C.T. Kowalski, "Dynamical performances of sensorless induction motor drive with different flux and speed observers", *Proc. 10^{th} Int. Conf. EPE'2001* 1, CD-ROM (2001).

[17] T. Orlowska-Kowalska and M. Dybkowski, "Dynamical properties of induction motor drive with novel MRAS estimator", *Electrical Review* 82 (11), 35–38 (2006).

[18] H. Kubota and Y. Tamura, "Stator resistance estimation for sensorless induction motor drives under regenerating condition", *Proc. IEEE Industrial Electronics Society Conf. IECON'2002* 1, 426–430 (2002).

[19] M. Saejia and S. Sangwongwanich, "Averaging analysis approach for stability analysis of speed-sensorless induction motor drives with stator resistance estimation", *IEEE Trans. Industrial Electronics* 53 (1), 163–177 (2006).

[20] T. Orlowska-Kowalska and M. Dybkowski, "Stator current-based mras estimator for a wide range speed-sensorless induction motor drive", *IEEE Trans. Industrial Electronics* 57 (4), 1296–1308 (2010).

[21] R.R. Yager and D.P. Filev, *Essentials of Fuzzy Modeling and Control*, John Wiley & Sons, New York, 1994.

[22] S. Bogosyan, M. Barut, and M. Gokasan, "Braided extended kalman filters for sensorless estimation in induction motors at high-low/zero speed", *IET Proc. – Control Theory and Applications* 1 (4), 987–998 (2007).

[23] T. Żabiński and L. Trybus, "Tuning P-PI and PI-PI controllers for electrical servos", *Bull Pol Ac.: Tech* 58 (1), 51–58 (2010).